NEUROSCIENCE

# An orbitofrontal cortex–anterior insular cortex circuit gates compulsive cocaine use

**Yang Chen[1,2]†, Guibin Wang[3]†, Wen Zhang[1], Ying Han[1], Libo Zhang[1,4], Hubo Xu[1], Shiqiu Meng[1], Lin Lu[1,5]*, Yanxue Xue[1,6,7]*, Jie Shi[1,4,6,8]***



**Compulsive drug use, a cardinal symptom of drug addiction, is characterized by persistent substance use despite adverse consequences. However, little is known about the neural circuit mechanisms behind this behavior. Using a footshock-punished cocaine self-administration procedure, we found individual variability of rats in the process of drug addiction, and rats with compulsive cocaine use presented increased neural activity of the anterior insular cortex (aIC) compared with noncompulsive rats. Chemogenetic manipulating activity of aIC neurons, especially aIC glutamatergic neurons, bidirectionally regulated compulsive cocaine intake. Furthermore, the aIC received inputs from the orbitofrontal cortex (OFC), and the OFC-aIC circuit was enhanced in rats with compulsive cocaine use. Suppression of the OFC-aIC circuit switched rats from punishment resistance to sensitivity, while potentiation of this circuit increased compulsive cocaine use. In conclusion, our results found that aIC glutamatergic neurons and the OFC-aIC circuit gated the shift from controlled to compulsive cocaine use, which could serve as potential therapeutic targets for drug addiction.**

## INTRODUCTION

Compulsive drug use, often accompanied by persistent drug use despite negative consequences, is one of the intractable features of addiction (*1*, *2*). Humans addicted to drugs are unable to shift their thoughts and behaviors away from drugs and drug-related things, even with awareness of the devastating effects on their personal and social well-being, and often in the face of danger and punishment by the legal system (*1*, *3*–*6*). Epidemiological studies showed that only a subset of drug users lost control over drug use and met the diagnostic criteria of addiction (*7*, *8*). This suggests that there must be individual differences in the development of drug addiction (*9*).

In previous studies, nearly all rodents learned to self-administer addictive drugs after self-administration training, including cocaine (*3*, *4*, *10*). In those experiments, most rodents stopped accessing cocaine when facing a noxious footshock as punishment simultaneously, whereas approximately 30% of rats persisted in getting cocaine, which mimicked compulsive drug use of humans in the clinic (*3*, *10*). This suggested that controlled and compulsive drug use were two distinct stages of addiction (*11*). Thus, treatment based on the animal models that only receive addictive substances might achieve limited effects due to confusing controlled with compulsive drug use (*11*, *12*). It is therefore important to disentangle the neural mechanisms behind compulsive drug use.

On the basis of neuroimaging, electroencephalogram, brain lesion, and pharmacological studies, the insular cortex (IC) has been found to be involved in some aspects of addiction, such as interoception, decision-making, anxiety, cognition, mood, and urges (*13*–*15*). Smokers with IC damage were more likely to undergo a disruption of smoking, characterized by the ability to quit smoking easily, and without persistence of the urge to smoke (*16*). However, whether and how IC is implicated in compulsive drug seeking remains elusive.

The IC is one of the most complex anatomical hubs in mammalian brain, including anterior IC (aIC) and posterior IC (pIC) (*17*). The pIC primarily connects with sensorimotor integration areas, which mainly plays a role in pain regulation (*18*). The aIC is functionally associated with limbic areas and regions comprising the "salience network" and serves cognitive functions such as behavioral motivation, which are compromised in drug addiction (*15*). Moreover, aIC connects with prefrontal cortex (PFC), orbitofrontal cortex (OFC), and amygdala (*17*), which have been reported to regulate compulsive drug use (*3*, *9*, *10*). A recent study reported that leptin-sensitive aIC pyramidal neurons modulated compulsive eating behavior, which shared many characteristics with compulsive drug use (*19*). However, the function of aIC in compulsive drug use behavior has not been investigated.

Here, we hypothesized that aIC and its associated circuit may be involved in compulsive cocaine use. In the present study, using a footshock-punished cocaine self-administration procedure combined with clustering analysis, immunostaining, fiber photometry, electrophysiology, and chemogenetics, we found that aIC glutamatergic neurons and OFC-aIC circuit played an important role in regulation of compulsive cocaine use, which provided a previously unidentified anatomical and functional circuit mediating drug addiction.

[1]National Institute on Drug Dependence and Beijing Key Laboratory of Drug Dependence, Peking University, Beijing 100191, China. [2]Department of Pharmacology, School of Basic Medical Sciences, Peking University Health Science Center, Beijing 100191, China. [3]Institute of Materia Medica, Chinese Academy of Medical Sciences & Peking Union Medical College, Beijing 100050, China. [4]Peking University Shenzhen Hospital, Shenzhen 518036, China. [5]Peking University Sixth Hospital, Peking University Institute of Mental Health, NHC Key Laboratory of Mental Health (Peking University), National Clinical Research Center for Mental Disorders (Peking University Sixth Hospital), Beijing 100191, China. [6]The Key Laboratory for Neuroscience of the Ministry of Education and Health, Peking University, Beijing 100191, China. [7]Chinese Institute for Brain Research, Beijing 102206, China. [8]The State Key Laboratory of Natural and Biomimetic Drugs, Peking University, Beijing 100191, China.
†These authors contributed equally to this work.
*Corresponding author. Email: shijie@bjmu.edu.cn (J.S.); yanxuexue@bjmu.edu.cn (Y.X.); linlu@bjmu.edu.cn (L.L.)

## RESULTS

### A subpopulation of rats displayed compulsive cocaine use behavior

Rats underwent 12 days of cocaine self-administration training with a fixed-ratio-1 (FR1) reinforcement procedure (Fig. 1A). Under these unpunished conditions, rats learned cocaine self-administration and cocaine infusions reached approximately 80 times per day in the last 3 days. Then, rats received 3 days of 1-hour punishment test in which each active nosepoke was paired with an additional footshock (0.25 mA, 0.5 s). An unsupervised clustering analysis (*20*) integrating four behavioral parameters (active nosepokes, inactive nosepokes, futile nosepokes, and cocaine infusions) over the last two punishment sessions (P2 and P3) yielded two clusters: shock-resistant and shock-sensitive rats (Fig. 1B). We found that 31 of 91 rats (34%) were classified as shock resistant, and 60 of 91 rats (66%) were classified as shock sensitive.

Facing noxious footshock, sensitive rats reduced cocaine self-administration quickly, while resistant rats kept using cocaine regardless of punishment (Fig. 1C). Cocaine use behaviors (Fig. 1, D and E), total cocaine intake during the acquisition sessions, and the break points in the progressive ratio test (fig. S1, A and B) were similar in both groups, suggesting that divergent responses to punishment were not influenced by the history of cocaine self-administration. The performance of extinction learning and the subsequent cue-induced reinstatement were also similar in two groups (fig. S1, C and D). Moreover, there was no difference in pain threshold between two groups of rats in hot plate test (fig. S1E), implying that different responses to punishment were not due to different pain sensitivity.

### The aIC neurons were hyperactive in shock-resistant rats

Next, we performed a c-Fos–based neural activity approach to examine the activity of aIC neurons in two groups of rats during punishment test. We also examined c-Fos expression in other brain regions that have been reported to be associated with drug addiction (*11*, *21*). Resistant rats presented an increased number of c-Fos–positive neurons in aIC, OFC, nucleus accumbens (NAc) shell, NAc core, dorsolateral striatum (DLS), and central amygdala (CeA)

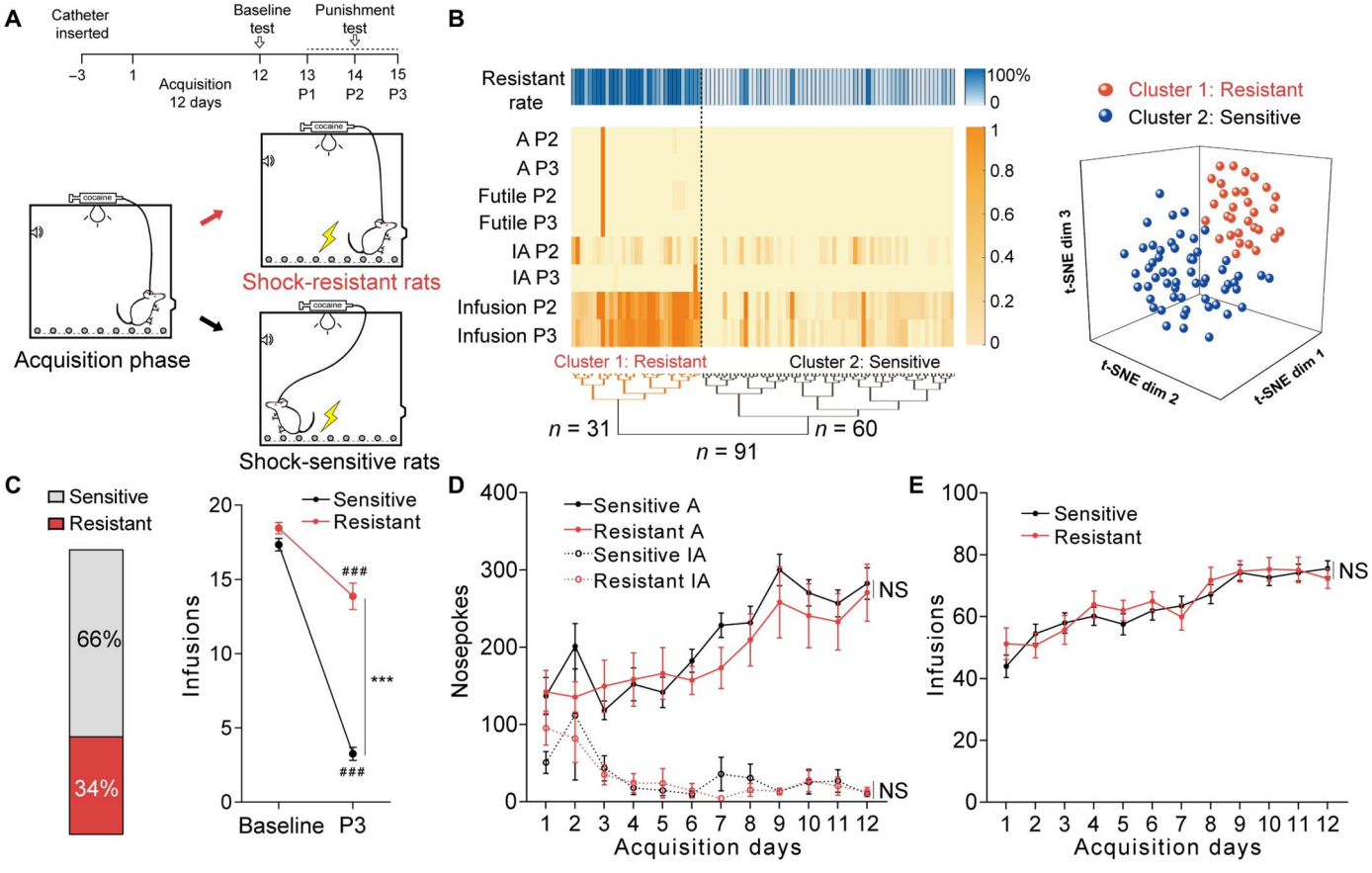


**Fig. 1. A subpopulation of rats displayed compulsive cocaine use behavior.** (**A**) Experimental timeline for identifying rats with compulsive cocaine use. (**B**) Hierarchical clustering based on *t*-distributed stochastic neighbor embedding (t-SNE) projection of parameters in punishment sessions 2 and 3 (P2 and P3) and t-SNE three-dimensional representation of clusters including resistant (cluster 1) and sensitive (cluster 2) rats. Behavioral performance included active nosepokes (A), inactive nosepokes (IA), futile nosepokes, and cocaine infusions. (**C**) Ratio of sensitive and resistant rats (left), and cocaine infusions obtained from baseline and the third punishment session (right). Sensitive rats had fewer infusions compared with resistant rats. Two-way analysis of variance (ANOVA) revealed a statistically significant interaction effect, $F_{1,89} = 80.76$, $P < 0.001$, post hoc analysis, $^{***}P < 0.001$ for sensitive versus resistant in P3, $^{###}P < 0.001$ for P3 versus baseline in sensitive or resistant group; $n = 60$ and 31, respectively. (**D** and **E**) Number of active nosepokes, inactive nosepokes, and cocaine infusions obtained from acquisition sessions. There was no difference between sensitive and resistant rats; two-way ANOVA showed nonsignificant main effects on groups, $F_{1,89} = 0.53$, $P = 0.4671$ for active nosepokes, $F_{1,89} = 0.03$, $P = 0.8639$ for inactive nosepokes, and $F_{1,89} = 0.14$, $P = 0.7086$ for infusions; $n = 60$ and 31, respectively. NS, not significant. Data are presented as mean values ± SEMs.

compared with sensitive rats (Fig. 2, A and B). Notably, neurons stained positively for c-Fos did not differentiate between resistant and sensitive rats in pIC, implying that pIC may be unrelated to compulsive cocaine use.

To further confirm the relationship between activated aIC neurons and compulsive cocaine use, we expressed calcium indicator GCaMP6f in aIC neurons and recorded in vivo calcium photometry signals during punishment test (Fig. 2C). Fiber photometry recordings were applied in three groups: resistant rats, sensitive rats, and cocaine-trained rats without punishment (no punish). Compared with the other two groups of rats, the activity of aIC neurons was increased when resistant rats continually got cocaine in punishment test (Fig. 2, D to F). Furthermore, we performed ex vivo electrophysiology to compare the spontaneous excitatory postsynaptic currents (sEPSCs) of aIC neurons between resistant and sensitive rats. The amplitude and frequency of sEPSCs were significantly increased in resistant rats compared with sensitive rats (Fig. 2G). Together, these results implied that cocaine self-administration under punishment was correlated with aIC neuron hyperactivity.

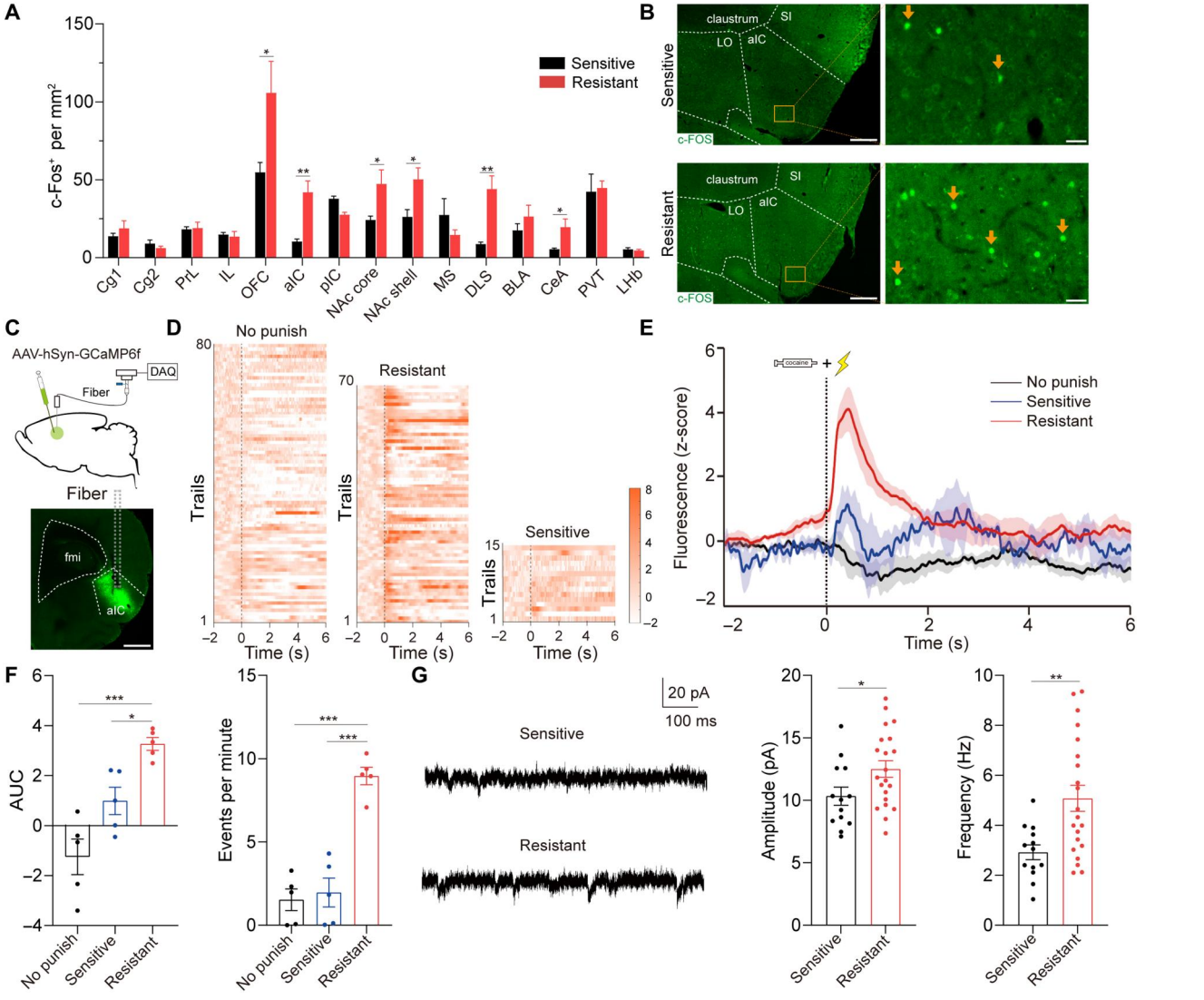


**Fig. 2. Hyperactive aIC neurons in shock-resistant rats.** (**A**) Mapping of c-Fos across brain regions 90 min after the third punishment test. Unpaired *t* test, $t_{11} = 2.24$, $^{*}P = 0.046$ for OFC; $t_{10} = 4.21$, $^{**}P = 0.005$ for aIC; $t_{12} = 2.50$, $^{*}P = 0.039$ for NAc core; $t_{12} = 2.53$, $^{*}P = 0.027$ for NAc shell; $t_{12} = 4.13$, $^{**}P = 0.004$ for DLS; $t_{12} = 2.71$, $^{*}P = 0.03$ for CeA; $n = 5$ to 6 and 7 to 8, respectively. (**B**) Representative images of c-Fos immunofluorescence staining of aIC. Scale bars, 500 μm (left) and 50 μm (right). (**C**) Schematic of calcium photometry. Scale bar, 1 mm. (**D** and **E**) Heatmap and plot of *z*-scored aIC $Ca^{2+}$ signals in no punish, sensitive, and resistant group; $n = 5$ for each group. (**F**) AUC of *z*-scored aIC $Ca^{2+}$ signals in 0 to 2 s. One-way ANOVA, $F_{2,12} = 17.58$, $P < 0.001$, post hoc analysis, $^{*}P = 0.028$ for sensitive versus resistant, $^{***}P < 0.001$ for no punish versus resistant. Number of events per minute of aIC neurons. One-way ANOVA, $F_{2,12} = 36.00$, $P < 0.001$, post hoc analysis, $^{***}P < 0.001$ for sensitive versus resistant and no punish versus resistant; $n = 5$ for each group. (**G**) Amplitude and frequency of sEPSCs of aIC neurons. Unpaired *t* test, $t_{32} = 2.12$, $^{*}P = 0.042$ and $t_{32} = 3.60$, $^{**}P = 0.001$, respectively; 13 neurons from 3 sensitive rats and 21 neurons from 5 resistant rats. Cg1, cingulate cortex area 1; Cg2, cingulate cortex area 2; PrL, prelimbic cortex; IL, infralimbic cortex; NAc core/shell, nucleus accumbens core/shell; MS, medial septum; DLS, dorsolateral striatum; BLA, basolateral amygdala; CeA, central amygdala; PVT, paraventricular thalamus; LHb, lateral habenula. Data are presented as mean values ± SEMs.

### Activation of aIC neurons was required and sufficient for compulsive cocaine use

To determine the causal link between enhanced aIC neuronal excitability and resistance to punishment, we inhibited aIC neurons through inhibitory designer receptor exclusively activated by designer drug (DREADD) hM4D via bilateral infusion of AAV-hSyn-hM4D-mCherry in aIC (Fig. 3A), which has been shown to be able to inhibit excitability of aIC neurons (fig. S3A). For control group, AAV-hSyn-mCherry was bilaterally infused into aIC. Seven days after viral infusion, rats received 12 days of cocaine self-administration training followed by punishment tests. An unbiased machine learning model was used to identify behavioral type of rats (see Materials and Methods). After the third punishment test, 10 of 28 (36%) rats were identified as resistant in control group and 10 of 31 (32%) rats were resistant in experimental group. After 2 days of recovery training, we inhibited aIC by intraperitoneal administration of clozapine *N*-oxide (6 mg/kg) 30 min before each punishment test (P4 to P6). After the sixth punishment test, 9 of 28 (32%) rats were identified as resistant rats in control group, while no resistant rats were identified in experimental group. Chemogenetic inhibition of aIC elicited a significant reduction of compulsive cocaine use among resistant rats, and all resistant rats restored sensitivity to punishment (Fig. 3, B and C). In contrast, inhibition of aIC among sensitive rats did not affect cocaine use in punishment test (fig. S4A). Furthermore, pain threshold and locomotor activity of rats were not changed after inhibition of aIC neurons (fig. S2, A to C), implying that reduced compulsive cocaine use was not due to change of pain threshold or locomotor activity.

To study whether activation of aIC neurons constituted a sufficient condition for compulsive cocaine use, AAV-hSyn-hM3D-mCherry was infused into aIC, allowing for the incorporation of excitatory DREADD in aIC neurons (Fig. 3D), which has been shown to be able to increase neuronal activity of aIC (fig. S3B). For control group, AAV-hSyn-mCherry was infused into aIC. Activation of aIC neurons increased compulsive cocaine infusions during punishment test, and 12 of 13 (92%) rats were identified as resistant in experimental group, while 5 of 14 (36%) rats were resistant in control group (Fig. 3, E and F). The pain threshold and locomotor activity of rats were not changed after activation of aIC neurons (fig. S2, C to E), indicating that increased compulsive cocaine use was not due to change of pain threshold or locomotor activity. Together, these

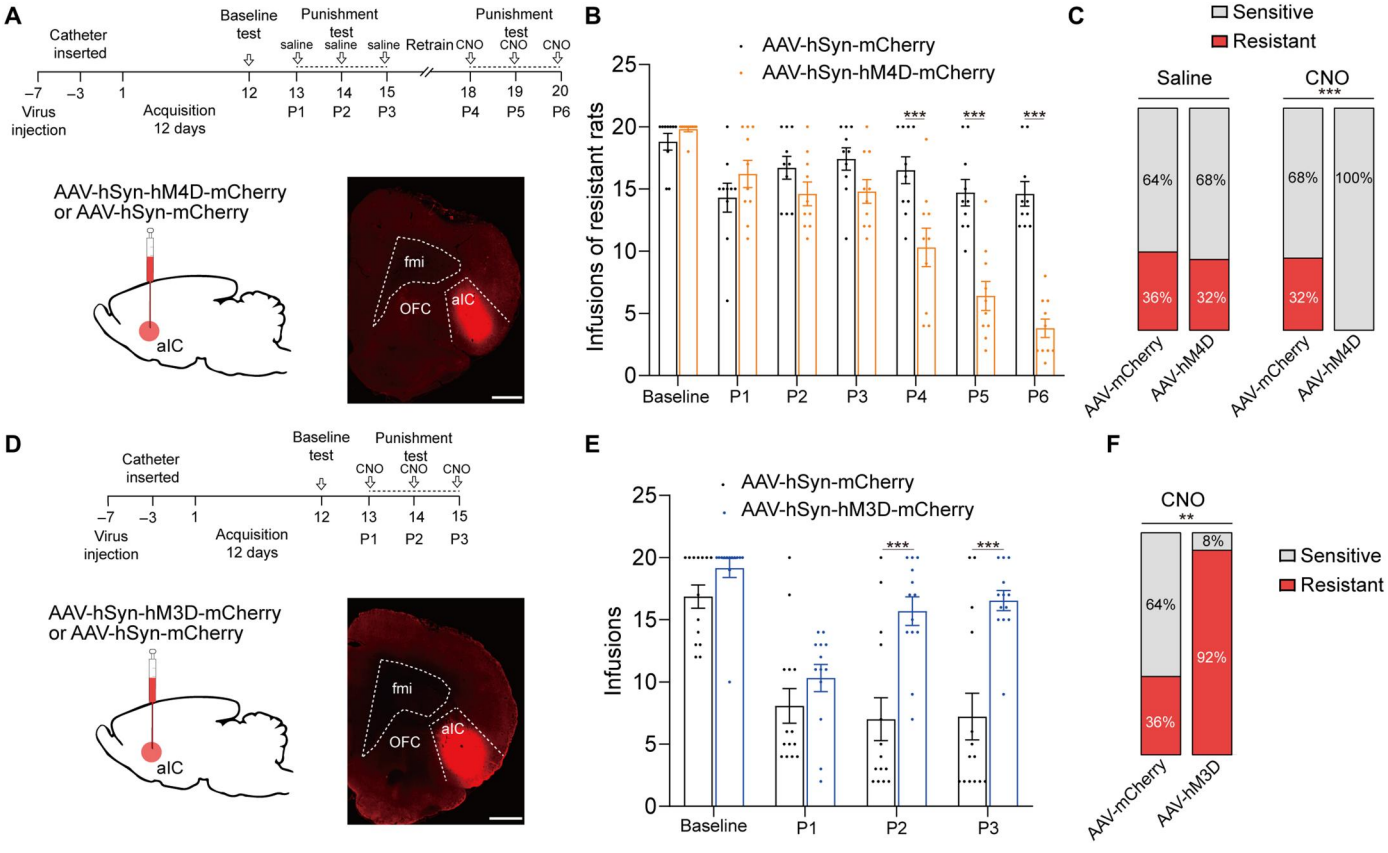


**Fig. 3. Activation of aIC neurons was required and sufficient for compulsive cocaine use.** (**A**) Experimental timeline and schematic of viral infusion to analyze compulsive cocaine use behavior after inhibition of aIC among resistant rats. Scale bar, 1 mm. (**B**) Cocaine infusions obtained from AAV-mCherry and AAV-hM4D group. Two-way ANOVA, $F_{1,18} = 22.51$, $P < 0.001$, post hoc analysis, ***$P < 0.001$ for P4, P5, and P6; $n = 10$ for each group. (**C**) Ratio of sensitive and resistant rats in AAV-mCherry and AAV-hM4D group before and after aIC inhibition; Fisher's exact test, ***$P < 0.001$. (**D**) Experimental timeline and schematic of viral infusion to analyze compulsive cocaine use behaviors after activation of aIC. Scale bar, 1 mm. (**E**) Cocaine infusion obtained from AAV-mCherry and AAV-hM3D group. Two-way ANOVA, $F_{1,25} = 15.22$, $P < 0.001$, post hoc analysis, ***$P < 0.001$ for P2 and P3; $n = 14$ and 13, respectively. (**F**) Ratio of sensitive and resistant rats in AAV-mCherry and AAV-hM3D group after aIC activation; Fisher's exact test, **$P = 0.004$. Data are presented as mean values ± SEMs.

findings indicated that activation of aIC was necessary and sufficient for compulsive cocaine use.

### The activity of aIC glutamatergic neurons bidirectionally modulated compulsive cocaine use

Since previous studies suggest that most aIC neurons are glutamatergic (*15*, *22*), we speculate that glutamatergic neurons of aIC play a role in modulation of compulsive cocaine use. To test our speculation, we inhibited aIC glutamatergic neurons by expressing calcium/calmodulin-dependent protein kinase IIα (CaMKIIα) promoter inhibitory DREADD via infusion of AAV-CaMKIIα-hM4D-mCherry into aIC (Fig. 4A). For control group, AAV-CaMKIIα-mCherry was infused into aIC. After the third punishment test, 10 of 32 (31%) and 8 of 29 (28%) rats were identified as resistant in control and experimental group, respectively. After the sixth punishment test, 10 of 32 (31%) rats were identified as resistant in control group, while no resistant rats were identified in experimental group, implying that chemogenetic inhibition of aIC glutamatergic neurons could reduce compulsive cocaine use (Fig. 4, B and C). In contrast, inhibition of aIC glutamatergic neurons among sensitive rats did not affect cocaine use in punishment test (fig. S4B).

Furthermore, we evaluated whether a gain function of aIC glutamatergic neurons might enhance compulsive drug use as nonspecific chemogenetic activation of aIC neurons. We expressed excitatory DREADD in aIC glutamatergic neurons via infusion of AAV-CaMKIIα-hM3D-mCherry (Fig. 4D). For control group, AAV-CaMKIIα-mCherry was infused into aIC. Activation of aIC glutamatergic neurons resulted in increased compulsive cocaine infusions and 12 of 14 (86%) rats were identified as resistant, while 4 of 12 (33%) rats were resistant in control group (Fig. 4, E and F). These data indicated that aIC glutamatergic neurons could bidirectionally regulate compulsive cocaine use.

### Potentiation of OFC-aIC circuit drove compulsive cocaine use

Next, we sought to identify aIC-related neural circuits participating in compulsive cocaine use. Previous studies found that chemogenetic and optogenetic activation of OFC could induce compulsive cocaine intake (*6*, *10*), and our results also showed the increased neural activity of OFC in resistant rats. In addition, the aIC received wide projections from cortical regions including the OFC (*17*), implying that the OFC-aIC pathway may play a role in compulsive cocaine use.

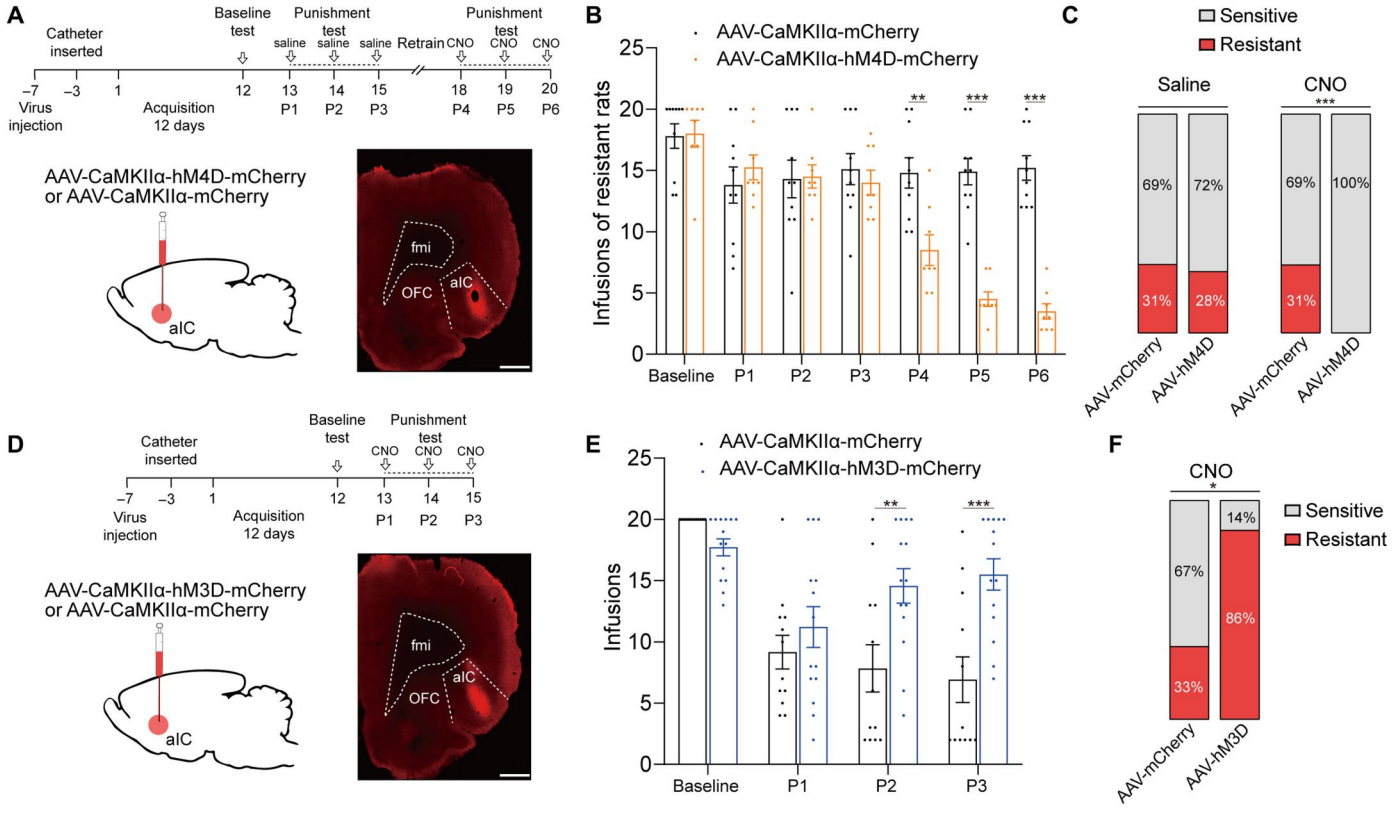


**Fig. 4. The aIC glutamatergic neurons bidirectionally modulated compulsive cocaine use.** (**A**) Experimental timeline and schematic of viral infusion to analyze compulsive cocaine use behaviors after inhibition of aIC glutamatergic neurons among resistant rats. Scale bar, 1 mm. (**B**) Cocaine infusions obtained from AAV-mCherry and AAV-hM4D group. Two-way ANOVA, $F_{1,16} = 9.89$, $P = 0.006$, post hoc analysis, $^{**}P = 0.001$ for P4, $^{***}P < 0.001$ for P5 and P6; $n = 10$ and 8, respectively. (**C**) Ratio of sensitive and resistant rats in AAV-mCherry and AAV-hM4D group before and after inhibition of aIC glutamatergic neurons; Fisher's exact test, $^{***}P < 0.001$. (**D**) Experimental timeline and schematic of viral infusion to analyze compulsive cocaine use behaviors after activation of aIC glutamatergic neurons. Scale bar, 1 mm. (**E**) Cocaine infusions obtained from AAV-mCherry and AAV-hM3D group. Two-way ANOVA, $F_{1,24} = 6.42$, $P = 0.018$, post hoc analysis, $^{**}P = 0.004$ for P2, $^{***}P < 0.001$ for P3; $n = 12$ and 14, respectively. (**F**) Ratio of sensitive and resistant rats in AAV-mCherry and AAV-hM3D group after activation of aIC glutamatergic neurons; Fisher's exact test, $^{*}P = 0.014$. Data are presented as mean values ± SEMs.

To anatomically confirm whether OFC neurons target aIC neurons, we first conducted retrograde tracing of aIC neurons by injecting cholera toxin B subunit (CTB) into aIC (fig. S5). We also used another tracing strategy that an anterograde adeno-associated viral vector ($AAV_{2/1}$-hSyn-Cre), which expressed Cre recombinase in postsynaptic neuronal targets, was infused into OFC, and then a Cre-dependent mCherry-expressing viral vector (AAV-EF1α-DIO-mCherry) was infused into aIC to further confirm afferents to aIC from OFC (Fig. 5A). These results confirmed that aIC received direct inputs from OFC.

To identify whether the OFC-aIC pathway was implicated in compulsive cocaine use, we compared excitatory synaptic transmission of labeled neurons in the OFC-aIC pathway between sensitive and resistant rats through viral vector system above. The amplitude and frequency of sEPSCs of these neurons were significantly increased in resistant rats compared with sensitive rats (Fig. 5B). Furthermore, we investigated the changes in neural activity of these neurons under current clamp. The input (the intensity of injection current)–output (spike number) curve obviously shifted to the left in resistant rats compared with sensitive rats (Fig. 5C), implying increased activity of OFC-aIC circuit in rats with compulsive cocaine use.

To confirm whether the increased sEPSCs of aIC neurons in resistant rats were derived from the OFC inputs, we probed the synaptic plasticity of OFC-aIC connections by measuring the paired-pulse ratio (PPR) and the AMPA/N-methyl-D-aspartate (NMDA) receptor (A/N) ratio. For this, OFC was infused with AAV-CaMKIIα-ChR2-mCherry, and we performed whole-cell patch-clamp recordings at aIC neurons that responded to a blue laser (470 nm, 1 to 3 mW) in no punish, sensitive, and resistant group, respectively (Fig. 5D). We found that the PPR of these aIC neurons receiving inputs from OFC was decreased, and the A/N ratio of these aIC neurons was increased in resistant group compared with no punish or sensitive group (Fig. 5, E to H). These results suggested that increased synaptic plasticity occurred at the OFC-aIC pathway of resistant rats instead of sensitive rats, and both presynaptic and postsynaptic mechanisms were involved in this process.

Most aIC neurons that received inputs from OFC were glutamatergic (Fig. 6A), and these aIC neurons had a higher colabeling ratio with c-Fos in resistant rats compared with that in sensitive rats (Fig. 6B). According to the function of aIC glutamatergic neurons in compulsive cocaine use behavior and the results from electrophysiological and immunofluorescence staining experiments above, we speculate that OFC-aIC might also play a role in this behavior. To test our hypothesis, we chemogenetically inhibited OFC-aIC circuit via infusion of $AAV_{2/1}$-hSyn-Cre into OFC and AAV-EF1α-DIO-hM4D-mCherry into aIC (Fig. 6C). For control group, $AAV_{2/1}$-hSyn-Cre was infused into OFC and AAV-EF1α-DIO-mCherry was infused into aIC. After the third punishment test, 9 of 32 (28%) and 9 of 30 (30%) rats were identified as resistant in control and experimental group, respectively. After the sixth punishment test, 10 of 32 (31%) rats were identified as resistant in control group, while no resistant rats were identified in experimental group. Chemogenetic inhibition of OFC-aIC circuit prevented compulsive cocaine use (Fig. 6D), and all resistant rats restored sensitivity to punishment (Fig. 6E). Among sensitive rats, inhibition of OFC-aIC circuit had no influence on cocaine use during punishment test (fig. S4C). These data suggested that activation of OFC-aIC circuit was necessary for compulsive cocaine use.

Next, we evaluated whether activation of OFC-aIC circuit was sufficient to drive compulsive cocaine use. For this, $AAV_{2/1}$-hSyn-Cre was infused into OFC and AAV-DIO-hM3D-mCherry was infused into aIC (Fig. 6F). For control group, $AAV_{2/1}$-hSyn-Cre was infused into OFC and AAV-DIO-mCherry was infused into aIC. Activation of OFC-aIC circuit resulted in increased compulsive cocaine infusions (Fig. 6G), and 12 of 15 (80%) of rats were identified as resistant in experimental group, while 3 of 9 (33%) rats were resistant in control group (Fig. 6H). This suggested that activation of OFC-aIC circuit was sufficient to induce compulsive cocaine use.

Furthermore, to test the specificity of OFC-aIC circuit in compulsive cocaine use, we evaluated whether a gain function of another aIC-related circuit could induce compulsive cocaine use. A previous study found that aIC also received input projections from cingulate cortex area 1 (Cg1) (*17*, *23*) (fig. S5), which showed a similar expression of c-Fos between sensitive and resistant rats (Fig. 2A). To test whether activation of Cg1-aIC circuit could induce compulsive cocaine use, $AAV_{2/1}$-hSyn-Cre was infused into Cg1 and AAV-DIO-hM3D-mCherry was infused into aIC (fig. S6A). Last, we found that compulsive cocaine use behavior and the percentage of resistant rats were not affected by Cg1-aIC circuit activation (fig. S6, B and C).

## DISCUSSION

The present study implies that increased activity of glutamatergic aIC neurons, especially those receiving afferent projections from OFC, gates the state of compulsive cocaine use (fig. S8). Approximately 30% of rats presented persistent cocaine use despite noxious footshock in our experiment, which was consistent with a previous study (*3*) and mimicked compulsive drug use in humans. The OFC (*6*, *20*), NAc shell and core (*24*–*26*), DLS (*27*), and CeA (*9*), which have been reported to be involved in compulsive drug use, were also activated in resistant rats in our study.

A previous study showed that bilateral anterior insula lesions prevented the development of schedule-induced polydipsia, a measure of compulsive behavior, and reduced the level of schedule-induced polydipsia in high compulsive rats (*28*). Structural magnetic resonance imaging found that higher compulsive drinking scores were associated with smaller aIC volumes and thinner aIC cortices in patients with alcohol dependence (*29*). A recent study showed that activation of the insula, as measured by c-Fos expression, occurred during aversion-resistant alcohol drinking (*30*). Our study demonstrated the causality between hyperactive aIC neurons and resistance to punishment during the development of compulsive cocaine use, which represented an important step in understanding the mechanisms of drug addiction. Together, our study suggested that aIC has been proposed as a neurobiological gate for the development of compulsive behavior and provided previously unidentified evidence of dissociation function between pIC and aIC.

The aIC, which contains interoceptive re-representations that substantialize all subjective feelings from the body and emotional awareness, is implicated in executive-function and impulse-control processes, such as decision making under risk, and specific motivational functions (*14*, *15*, *31*–*33*). Together with previous findings, we speculated that aIC hyperactivity may magnify incentive representation of "feelings" of drugs and drug-related stimulation, and discount risk representation of negative consequences to

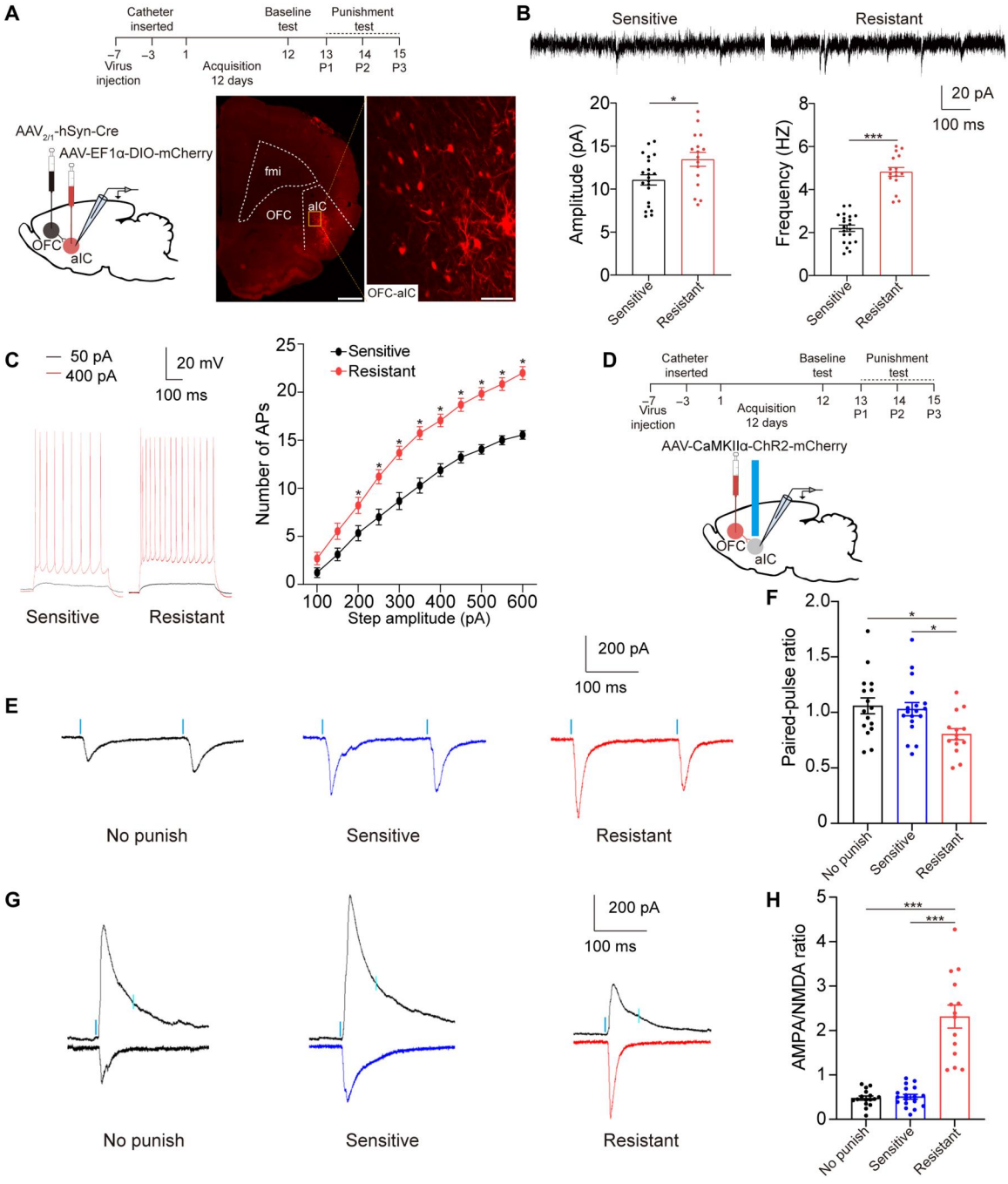


**Fig. 5. Glutamatergic projections from OFC to aIC were potentiated in resistant rats.** (**A**) Experimental timeline and schematic of whole-cell patch-clamp recordings of aIC neurons that received inputs from OFC. Scale bars, 1 mm (left) and 100 μm (right). (**B**) Amplitude and frequency of sEPSCs recorded from OFC-aIC neurons. Unpaired *t* test, $t_{35} = 2.42$, $^{*}P = 0.021$ for amplitude; $t_{35} = 10.71$, $^{***}P < 0.001$ for frequency, 21 neurons from four sensitive rats and 16 neurons from four resistant rats. (**C**) Number of APs responding to increasing step current obtained from aIC neurons that received inputs from OFC. Two-way ANOVA, $F_{1,187} = 297.4$, $P < 0.001$, post hoc analysis, $^{*}P < 0.05$ for 200 to 600 pA, 18 neurons from four sensitive rats and 19 neurons from three resistant rats. (**D**) Experimental timeline and schematic of whole-cell patch-clamp recordings of aIC neurons responding to a 470-nm laser (2 ms, blue bars). (**E** and **F**) The PPR of aIC neurons was significantly decreased in resistant rats compared with that in no punish and sensitive rats. One-way ANOVA, $F_{2,45} = 4.66$, $P = 0.0145$, post hoc analysis, $^{*}P = 0.0375$ for sensitive versus resistant, and $^{*}P = 0.0199$ for no punish versus resistant. (**G** and **H**) The A/N ratio of aIC neurons was significantly increased in resistant rats. One-way ANOVA, $F_{2,45} = 54.36$, $P < 0.001$, post hoc analysis, $^{***}P < 0.001$ for sensitive versus resistant and no punish versus resistant; 16 neurons from three no punish rats, 18 neurons from three sensitive rats, and 14 neurons from three resistant rats. Data are presented as mean values ± SEMs.

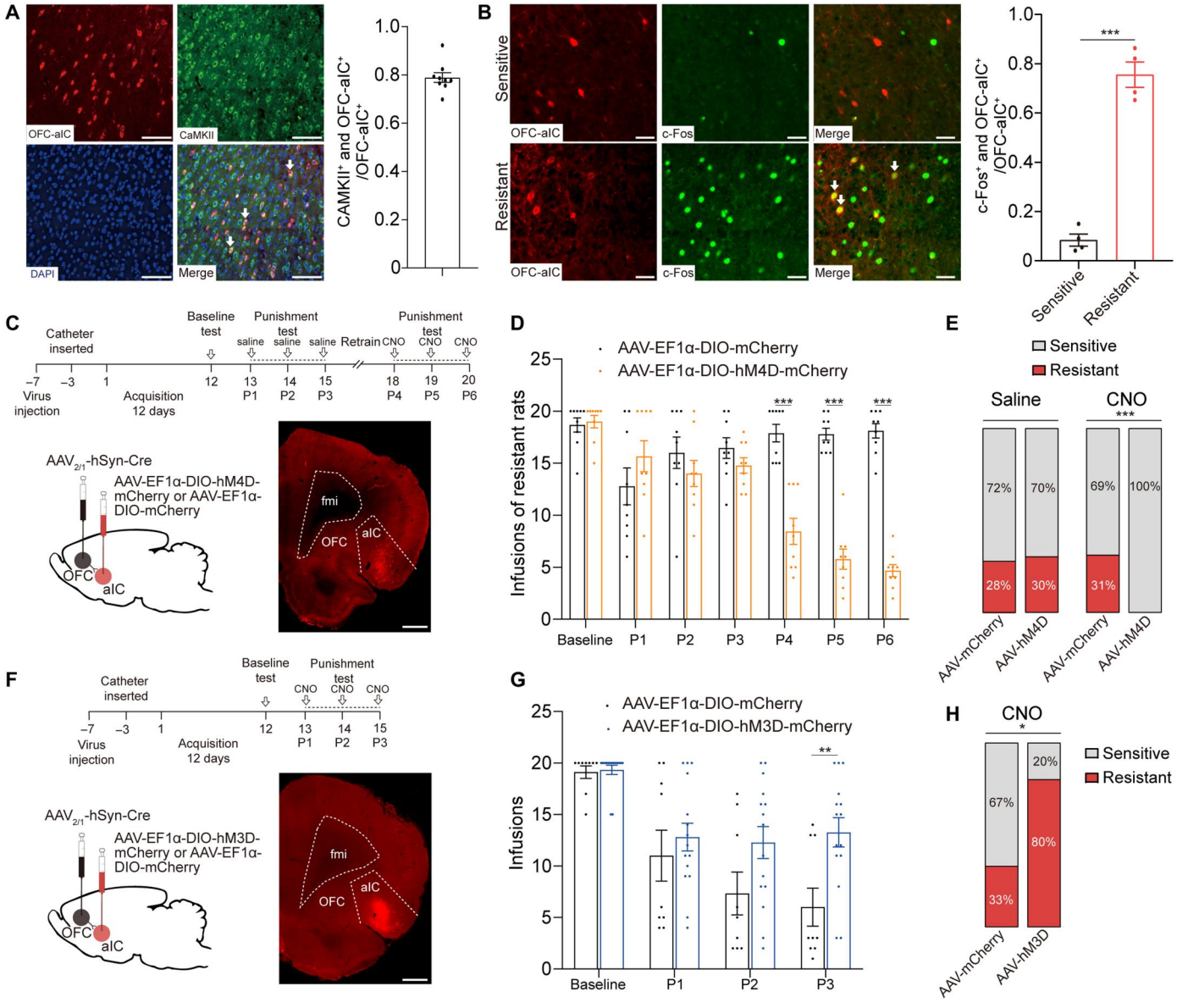


**Fig. 6. Potentiation of OFC-aIC circuit drove compulsive cocaine use.** (**A**) Representative double immunofluorescence labeling images of CaMKII and OFC-aIC neurons in aIC. Most of aIC neurons, which received inputs from OFC, were glutamatergic (CaMKII$^+$ and OFC-aIC$^+$/OFC-aIC$^+$ = 0.79); $n = 9$. Scale bar, 100 μm. (**B**) Representative double-labeling immunofluorescent images in sensitive (top) and resistant (bottom) rats and colocalization ratio of c-Fos and OFC-aIC neurons. The OFC-aIC neurons were significantly activated in resistant rats (0.08 versus 0.76 for sensitive and resistant rats). Unpaired $t$ test, $t_6 = 11.79$, ***$P < 0.001$, $n = 4$ for each group. Scale bar, 50 μm. (**C**) Experimental timeline and schematic of viral infusion to analyze compulsive cocaine use behaviors after inhibition of OFC-aIC circuit. Scale bar, 1 mm. (**D**) Cocaine infusions obtained from AAV-mCherry and AAV-hM4D group. Two-way ANOVA, $F_{1,16} = 38.95$, $P < 0.001$, post hoc analysis, ***$P < 0.001$ for P4, P5, and P6; $n = 9$ for each group. (**E**) Ratio of sensitive and resistant rats in AAV-mCherry and AAV-hM4D group before and after inhibition of OFC-aIC circuit; Fisher's exact test, ***$P < 0.001$. (**F**) Experimental timeline and schematic of viral infusion to analyze compulsive cocaine use behaviors after activation of OFC-aIC circuit. Scale bar, 1 mm. (**G**) Cocaine infusions obtained from AAV-mCherry and AAV-hM3D group. Two-way ANOVA, $F_{1,22} = 4.20$, $P = 0.053$, post hoc analysis, **$P = 0.005$ for P3; $n = 9$ and 15, respectively. (**H**) Ratio of sensitive and resistant rats in AAV-mCherry and AAV-hM3D group before and after activation of OFC-aIC circuit; Fisher's exact test, *$P = 0.036$. Data are presented as mean values ± SEMs.

drive compulsive cocaine seeking by encoding anticipation of reward (*21*), reward-based salience (*34*), punishment prediction errors (*35*), and risk taking (*36*).

We selectively targeted glutamatergic neurons of aIC, and their inhibition has been reported to prevent the formation of conditioned aversion (*37*). Our result implies that aIC glutamatergic neurons encode not only aversion but also reward; thus, inhibition of aIC glutamatergic neurons may suppress cocaine reward and prevent self-administration of cocaine facing punishment. Previous studies have found that perineuronal nets and alpha-1 noradrenergic receptor in the aIC could regulate compulsive alcohol drinking

(*30*, *38*), but how the two molecules modulate the excitability of glutamatergic neurons requires further exploration.

The OFC, which encodes the expected relative outcome value by updating previous information on reward and punishment reception (*39*, *40*), emerges as one of the hubs for compulsive reinforcement. Neuroimaging studies identified the changes of structural or functional connectivity between OFC and IC in nicotine- and alcohol-dependent patients, which were correlated with clinical symptoms of addiction (*41*–*43*). In addition, psychophysiological interaction analysis using left IC as a seed showed stronger connectivity with OFC during smoking cues compared with food cues (*44*). Our study reported a detailed role of OFC-IC circuit in drug addiction, suggesting that this circuit may serve as a key point to regulate compulsive cocaine use.

The projection from OFC to the dorsal striatum is widely believed to drive compulsive behavior (*6*, *20*). In rats showing compulsive methamphetamine taking, there is an imbalance in activity of different corticostriatal circuits, with more activity in OFC-DMS "go" circuit and less engagement of prelimbic cortex-ventrolateral striatal "stop" circuit (*45*). Our results demonstrate that OFC-aIC may be another go circuit, and its excitation may disrupt the balance of go and stop in the direction of driving compulsive cocaine use. Given the likely function of OFC in value updating and cost-benefit decision-making (*46*–*48*), we speculate that impaired decision-making underlain by an enhanced OFC-aIC circuit might differentiate the rats of those resistant to punishment from those sensitive rats during cocaine administration. Our results rule out the role of Cg1-aIC circuit in compulsive cocaine use. However, the current data could not fully exclude a small number of aIC-OFC projections and the other aIC-related pathways, such as amygdala to aIC projections (*49*), which might also contribute to compulsive cocaine use.

In conclusion, this study demonstrated the gating role of aIC glutamatergic neurons and OFC-aIC circuit in regulation of compulsive cocaine use, providing an explanation for patients with insula damage quitted smoking easily (*16*). Our findings might shed light on the understanding of compulsive drug use behavior and the development of related therapies for drug addiction.

## MATERIALS AND METHODS

### Animals

Adult male Sprague-Dawley rats (280 to 300 g) were purchased from Beijing Vital River Laboratory Animal Technology Co. Ltd. The rats were housed in groups of four per cage after arrival and individually housed after surgery with appropriate temperature (22 ± 2°C) and humidity (50 ± 5%), as well as freely accessible water and food. The lighting time was controlled under a 12-hour light/dark cycle. All behavioral experiments were performed during the animal's dark period. Animal care and experimentation were performed in accordance with the National Institutes of Health *Guide for the Care and Use of Laboratory Animals* and were approved by the Biomedical Ethics Committee for Animal Use and Protection of Peking University.

### Stereotaxic surgeries

Rats were deeply anesthetized using isoflurane. Then, rats were placed in a stereotaxic apparatus. The solution of virus was infused with a glass pipette. The volume of virus per injection site was 400 nl. After injection, the pipette was left in the injection site for an additional 10 min to allow diffusion of the viral particles.

For chemogenetic experiments, AAV-hSyn-hM3D(Gq)-mCherry-WPRE-PA, AAV-hSyn-hM4D(Gi)-mCherry-WPRE-PA, AAV-hSyn-mCherry-WPRE-PA, AAV-CaMKIIα-hM3D(Gq)-mCherry-WPRE-PA, AAV-CaMKIIα-hM4D(Gi)-mCherry-WPRE-PA, or AAV-CaMKIIα-mCherry-WPRE-PA was bilaterally infused into the aIC [anteroposterior (AP), +2.3; mediolateral (ML), ±5.0; dorsoventral (DV), −6.2 mm] (*50*). To monitor the neural activity of aIC during punishment test, aIC was infused with AAV-hSyn-GCaMP6f-WPRE-PA. An optic fiber (core diameter, 200 μm; length, 6 mm; numerical aperture, 0.37; Inper, Hangzhou, China) was inserted 0.2 mm above the injection site of the aIC. For optogenetic stimulation of aIC neurons that received glutamatergic inputs from OFC, AAV-CaMKIIα-ChR2-mCherry-WPRE-PA was infused into OFC (AP, +3.5; ML, ±2.1; DV, −4.4 mm) (*6*).

To label OFC-aIC circuit (*43*), anterograde trans-synaptic $AAV_{2/1}$-hSyn-Cre was bilaterally infused into the OFC (*6*) and AAV-EF1α-DIO-mCherry-WPRE-PA was bilaterally infused into aIC. To retrogradely label aIC (*33*), CTB-555 was infused into the unilateral aIC. For chemogenetic regulation of OFC-aIC circuit, $AAV_{2/1}$-hSyn-Cre was bilaterally infused into OFC followed by bilateral infusion of AAV-EF1α-DIO-hM4D(Gi)-mCherry-WPRE-PA, AAV-EF1α-DIO-hM3D(Gq)-mCherry-WPRE-PA, or AAV-EF1α-DIO-mCherry-WPRE-PA in aIC before catheter implantation. For chemogenetic regulation of Cg1-aIC circuit (*23*), $AAV_{2/1}$-hSyn-Cre was bilaterally infused in the Cg1 (AP, +3.7; ML, ±0.4; DV, −1.0 mm) followed by bilateral injection of AAV-EF1α-DIO-hM3D(Gq)-mCherry-WPRE-PA or AAV-EF1α-DIO-mCherry-WPRE-PA in aIC before catheter implantation. Moreover, we validated the accuracy of the OFC-aIC and Cg1-aIC labeling (fig. S7, A to D).

All viruses were provided by BrainVTA (Wuhan, China), and final viral titers were in the range of $1 \times 10^{12}$ to $5 \times 10^{12}$ viral particles per milliliter. All viruses were stored at −80°C. The rats were allowed to recover from the surgery for 3 to 5 days in their home cages.

### Catheter implantation

Rats were anesthetized through isoflurane, and then the catheter was placed into the right external jugular vein as our previous study (*51*). Then, another tip of catheter was passed under the skin of the neck to connect with cannula (Plastics-One) and finally fixed on the skull with dental cement. The catheter was flushed daily with a saline solution containing gentamicin (5 mg/ml) to help maintain catheter patency and reduce infection. Following surgery, rats were single-housed and allowed to recover for 3 to 5 days (*3*).

### Cocaine self-administration training

#### *Acquisition*

The chambers (AniLab Software and Instruments) were equipped with two nosepoke holes: one was active nosepoke, and the other was inactive nosepoke. The rats were trained in different chambers under an FR1 schedule of cocaine self-administration for 12 days (*51*). Daily cocaine self-administration training consists of six 1-hour sessions, and there is a 5-min interval between each session. Poking to the active nosepoke led to a cocaine infusion (0.75 mg/kg). There was a 20-s timeout phase between each infusion. The number of active nosepokes, inactive nosepokes, and cocaine

infusions was recorded. To prevent rats administrating overdose of cocaine, the number of infusions was limited to 20 times in each session.

***Punishment test***

Punishment test was performed according to previous studies with a few modifications (*5*, *6*). After 12 days of cocaine self-administration training, rat received 1-hour punishment session for three consecutive days. The baseline behavior was obtained from the last training day within the first hour. The punishment sessions were the same as training sessions except that rat received a mild footshock (0.25 mA, 0.5 s) paired with each cocaine infusion (*3*). The number of infusions was also limited to 20 times during punishment test to prevent overdose of cocaine.

***Progressive ratio test***

After the acquisition sessions, the rat underwent a progressive ratio test to measure the motivation of cocaine and the session of test lasted for 2 hours. The breakpoint was the cumulative number of nosepokes that the rat performed before it ceased poking after 40 min without receiving cocaine infusion. The reinforced schedules were according to the following progression: 1, 3, 5, 8, 12, 16, 22, 29, 38, 50, 65, 84, 108, 139, 178, 228, 291, 371, 473, 603, 767, 977, 1243, and 1582 (*6*).

***Extinction and reinstatement test***

After punishment test, the rat was subjected to an extinction session (6 hours) in previous chambers for 7 days without any cocaine infusions (*51*). During extinction, the conditions were the same as training except that drug was no longer available; that is, nosepoke responses led to a 5-s tone-light cue under an FR1 20-s timeout reinforcement schedule. Following extinction, the tone cue was used to challenge rat in the previous chamber for 1 hour and the number of active nosepokes was recorded during test.

## Hot plate test

The rat was placed on a metal surface (<42°C) of hot plate, and the temperature was increased at a constant rate (3.3°C/min) until nocifensive behavior was observed. The temperature of hind paw withdrawal was designated as thermal pain threshold (*52*).

## Locomotor activity

Locomotor activity test was conducted on the basis of previous studies (*53*, *54*). In this test, the rat was placed in the locomotor chamber (40 cm × 40 cm × 65 cm) and locomotor activity was recorded for 2 hours. All locomotor activities were recorded and analyzed with an automated video tracking system (DigBehv-LM4; Shanghai Jiliang Software Technology, Shanghai, China). Locomotor activity is expressed as the total distance traveled in centimeters during a predetermined period of time.

## Fiber photometry

We used single-channel fiber photometry system provided by Thinker Tech (Nanjing, China) (*55*). The 488-nm excitation light from a semiconductor laser (Coherent, OBIS 488 LS, tunable power up to 50 mW) was reflected by a dichroic mirror with a 452- to 490-nm reflection band and a 505- to 800-nm transmission band (Thorlabs, MD498) and then coupled to a fiber by an objective. The emission fluorescence was detected by a photomultiplier tube (Hamamatsu, H10720-210) after filtering by a green fluorescent protein bandpass emission filter (Thorlabs, MF525-39). The analog fluorescence data were streamed into a DAQ card (National Instruments, USB-6001), and signal was filtered by a low-pass filter (cutoff frequency, 30 Hz) and saved on the computer. The sampling rate was set to 100 Hz.

The fluorescence data were collected from no punish, sensitive, and resistant rats in each test for 1 hour. Analysis was performed in MATLAB, and we calculated the *z* score using the mean and SD of the signals (*55*). Area under the curve (AUC) was calculated as the integral between 0 and 2 s (*56*). Significant calcium events were identified as periods of time in which $\Delta F/F$ rose above 2.91 median absolute deviations (MADs) from baseline and remained at least two MADs above baseline (*57*). The event frequency was obtained from total number of identified events divided by duration of time during punishment sessions.

## Electrophysiology

Whole-cell patch-clamp recordings of aIC neurons were performed 24 hours after the last punishment session. The brains were rapidly removed after anesthetization, and 250-μm coronal slices were prepared with a vibratome (Leica VT1200S) in ice-cold solution containing 80 mM NaCl, 26 mM $NaHCO_3$, 3.0 mM KCl, 1.0 mM $NaH_2PO_4$, 1.3 mM $MgCl_2$, 1.0 mM $CaCl_2$, 20 mM D-glucose, and 75 mM sucrose, saturated with 95% $O_2$ and 5% $CO_2$. The slices were moved to an incubation chamber containing artificial cerebrospinal fluid containing 124 mM NaCl, 26 mM $NaHCO_3$, 3.0 mM KCl, 1.0 mM $NaH_2PO_4$, 1.3 mM $MgCl_2$, 1.5 mM $CaCl_2$, and 20 mM D-glucose, saturated with 95% $O_2$ and 5% $CO_2$ at 34°C for 30 min and then at room temperature until used for recording.

The potassium-based intracellular solution within the micropipettes (8 to 10 megohms) contained the following: 120 mM K-gluconate, 10 mM KCl, 4 mM adenosine 5′-triphosphate–Mg, 0.3 mM guanosine 5′-triphosphate, 10 mM Hepes, and 0.5 mM EGTA (pH 7.2, 270 to 280 mOsm). sEPSCs were recorded with membrane clamped at −60 mV and recorded for 3 min. To investigate the relationship between the spike number and the intensity of injected currents, neurons were current-clamped and injected 50- to 600-pA depolarizing currents with a step size of 50 pA (*50*).

To identify excitatory synaptic transmission of aIC neurons that received inputs from OFC, $AAV_{2/1}$-hSyn-Cre was infused into OFC and AAV-EF1α-DIO-mCherry was infused into aIC before cocaine self-administration training. After the last punished session, whole-cell patch-clamp recordings were performed in aIC neurons expressing red fluorescence, which were confirmed under a fluorescence microscope before recording.

The A/N ratio was estimated by calculating AMPAR-mediated EPSC amplitude (estimated as the optically evoked peak EPSC amplitude at a holding potential of −60 mV) divided by NMDA receptor–mediated EPSC amplitude (EPSC amplitude at a holding potential of 40 mV measured 65 to 70 ms after optostimulation). The PPR is the ratio of the optically evoked EPSC amplitude of the second response to that of the first with a 200-ms interval (holding at −60 mV). Blue light (470 nm, 1 to 3 mW, 2 ms) was applied through a 40× objective placed over the field of view of the patched cell.

Signals were amplified (Multiclamp 700B, Axon Instruments), filtered at 5 kHz, and digitized at 20 kHz (National Instruments Board PCI-MIO-16E4, Igor, Wave Metrics). Data were recorded within Axon pClamp 10 (Molecular Devices, CA 95134 USA). The methods of data analysis were described in our previous study (*58*).

### Clustering analysis

Clustering analysis was performed with Python. Before clustering, the eight variables of each rat were normalized by the model "preprocessing.MinMaxScaler" of "sklearn" in Python. The eight variables included active nosepokes (A), futile nosepokes, inactive nosepokes (IA), and cocaine infusions obtained from the last two punishment sessions (P2 and P3). Futile nosepokes were defined as active nosepokes during the 20-s timeout, which reflected the level of rat impulsion. A dimension reduction ("tsne" of "sklearn.manifold;" dimension number, 3) was applied to the eight normalized variables. The three dimensions were clustered by "Agglomerative Clustering" of "sklearn.cluster." Last, two clusters were defined as resistant and sensitive (*20*).

To eliminate the effect of sample size in different experiments on the cluster analysis (*20*), a machine learning–based predictive model was established to identify whether rats have developed into compulsive cocaine use. The matrix containing the eight variables of 91 rats in P2 and P3 was trained using linear kernel of MATLAB to predict the behavioral type of rats obtained from clustering analysis. The model was trained until the loss rate dropped below 10% in cross-validation analysis. Last, the model was used to predict behavioral type of rats according to its eight variables obtained from P2–3 or P5–6 in the following experiments except for the first behavioral experiment.

### Immunostaining

Immunostaining was performed as described in our previous study (*54*). The brains were fixed with 4% paraformaldehyde and transferred into phosphate-buffered saline (PBS; pH 7.2) containing 10, 20, and 30% sucrose until they sank. Slices were washed with PBS, blocked with 5% bovine serum albumin dissolved in 0.2% Triton X-100 for 1 hour at room temperature, and then incubated with primary antibodies, including rabbit anti–c-Fos (1:500, Abcam, ab190289) or mouse anti-CaMKII (1:500, Abcam, ab171095), which were dissolved in blocking buffer overnight at 4°C, followed by washing with PBS. Then, slices were incubated with fluorescent-conjugated secondary antibodies, including goat anti-rabbit secondary antibody (Alexa Fluor 488, 1:500, Invitrogen, A-11008) or donkey anti-mouse secondary antibody (Alexa Fluor 488, 1:500, Invitrogen, A-32766), which were dissolved in blocking buffer for 2 hours at room temperature followed by washing with PBS. Last, the slices were mounted with mounting medium containing 4′,6-diamidino-2-phenylindole (Abcam, ab285390) and stored at 4°C for further analysis.

Fluorescent images were acquired using a fluorescence microscope (Olympus, Tokyo, Japan) with a 20× objective lens and analyzed according to our previous studies (*51*, *54*). The size of sampled areas for cell quantifications of each brain region from each section was $0.33 \times 0.30$ mm$^2$. The c-Fos protein was identified and counted in IMARIS software (Oxford Instruments). An investigator blinded to the experimental conditions performed the image analyses.

### Statistical analysis

Statistical analyses were performed with GraphPad Prism 9. One-way analysis of variance (ANOVA), two-way ANOVA, or Student's *t* test was used to analyze the data. A nonparametric test was used if data did not meet a Gaussian distribution. Bonferroni test was used for post hoc analysis after ANOVA. Data were presented as mean ± SEM. Statistical details were presented in the figure legends. Significance was defined as $^*P < 0.05$, $^{**}P < 0.01$, and $^{***}P < 0.001$. Rats were randomly assigned to each group. The behavioral data were replicated in at least two batches of animals.

## Supplementary Materials

**This PDF file includes:**

Figs. S1 to S8

View/request a protocol for this paper from *Bio-protocol*.

## REFERENCES AND NOTES


1. L. J. Vanderschuren, B. J. Everitt, Drug seeking becomes compulsive after prolonged cocaine self-administration. *Science* **305**, 1017–1019 (2004).
2. American Psychiatric Association, *Diagnostic and Statistical Manual for Mental Disorders* (American Psychiatric Association, ed. 5, 2013); www.dsm5.org/Pages/Default.aspx.
3. B. T. Chen, H. J. Yau, C. Hatch, I. Kusumoto-Yoshida, S. L. Cho, F. W. Hopf, A. Bonci, Rescuing cocaine-induced prefrontal cortex hypoactivity prevents compulsive cocaine seeking. *Nature* **496**, 359–362 (2013).
4. B. J. Everitt, T. W. Robbins, Drug addiction: Updating actions to habits to compulsions ten years on. *Annu. Rev. Psychol.* **67**, 23–50 (2016).
5. N. J. Marchant, E. J. Campbell, K. Kaganovsky, Punishment of alcohol-reinforced responding in alcohol preferring P rats reveals a bimodal population: Implications for models of compulsive drug seeking. *Prog. Neuropsychopharmacol. Biol. Psychiatry* **87**, 68–77 (2018).
6. V. Pascoli, A. Hiver, R. Van Zessen, M. Loureiro, R. Achargui, M. Harada, J. Flakowski, C. Luscher, Stochastic synaptic plasticity underlying compulsion in a model of addiction. *Nature* **564**, 366–371 (2018).
7. B. F. Grant, R. B. Goldstein, T. D. Saha, S. P. Chou, J. Jung, H. Zhang, R. P. Pickering, W. J. Ruan, S. M. Smith, B. Huang, D. S. Hasin, Epidemiology of DSM-5 alcohol use disorder: Results from the National Epidemiologic Survey on Alcohol and Related Conditions III. *JAMA Psychiat.* **72**, 757–766 (2015).
8. F. A. Wagner, J. C. Anthony, From first drug use to drug dependence; developmental periods of risk for dependence upon marijuana, cocaine, and alcohol. *Neuropsychopharmacology* **26**, 479–488 (2002).
9. E. Augier, E. Barbier, R. S. Dulman, V. Licheri, G. Augier, E. Domi, R. Barchiesi, S. Farris, D. Natt, R. D. Mayfield, L. Adermark, M. Heilig, A molecular mechanism for choosing alcohol over an alternative reward. *Science* **360**, 1321–1326 (2018).
10. V. Pascoli, J. Terrier, A. Hiver, C. Luscher, Sufficiency of mesolimbic dopamine neuron stimulation for the progression to addiction. *Neuron* **88**, 1054–1066 (2015).
11. P. V. Piazza, V. Deroche-Gamonet, A multistep general theory of transition to addiction. *Psychopharmacology* **229**, 387–413 (2013).
12. C. Luscher, T. W. Robbins, B. J. Everitt, The transition to compulsion in addiction. *Nat. Rev. Neurosci.* **21**, 247–263 (2020).
13. M. Contreras, P. Billeke, S. Vicencio, C. Madrid, G. Perdomo, M. Gonzalez, F. Torrealba, A role for the insular cortex in long-term memory for context-evoked drug craving in rats. *Neuropsychopharmacology* **37**, 2101–2108 (2012).
14. N. H. Naqvi, N. Gaznick, D. Tranel, A. Bechara, The insula: A critical neural substrate for craving and drug seeking under conflict and risk. *Ann. N. Y. Acad. Sci.* **1316**, 53–70 (2014).
15. H. Deng, X. Xiao, T. Yang, K. Ritola, A. Hantman, Y. Li, Z. J. Huang, B. Li, A genetically defined insula-brainstem circuit selectively controls motivational vigor. *Cell* **184**, 6344–6360.e18 (2021).
16. N. H. Naqvi, D. Rudrauf, H. Damasio, A. Bechara, Damage to the insula disrupts addiction to cigarette smoking. *Science* **315**, 531–534 (2007).
17. D. A. Gehrlach, C. Weiand, T. N. Gaitanos, E. Cho, A. S. Klein, A. A. Hennrich, K. K. Conzelmann, N. Gogolla, A whole-brain connectivity map of mouse insular cortex. *eLife* **9**, e55585 (2020).
18. D. A. Gehrlach, N. Dolensek, A. S. Klein, R. Roy Chowdhury, A. Matthys, M. Junghänel, T. N. Gaitanos, A. Podgornik, T. D. Black, N. Reddy Vaka, K. K. Conzelmann, N. Gogolla, Aversive state processing in the posterior insular cortex. *Nat. Neurosci.* **22**, 1424–1437 (2019).
19. D. Kirson, S. R. Spierling Bagsic, J. Murphy, H. Chang, R. Vlkolinsky, S. N. Pucci, J. Prinzi, C. A. Williams, S. Y. Fang, M. Roberto, E. P. Zorrilla, Decreased excitability of leptin-sensitive anterior insula pyramidal neurons in a rat model of compulsive food demand. *Neuropharmacology* **208**, 108980 (2022).

20. Y. Li, L. D. Simmler, R. Van Zessen, J. Flakowski, J. X. Wan, F. Deng, Y. L. Li, K. M. Nautiyal, V. Pascoli, C. Luscher, Synaptic mechanism underlying serotonin modulation of transition to cocaine addiction. *Science* **373**, 1252–1256 (2021).
21. N. Apaydin, S. Ustun, E. H. Kale, I. Celikag, H. D. Ozguven, B. Baskak, M. Cicek, Neural mechanisms underlying time perception and reward anticipation. *Front. Hum. Neurosci.* **12**, 115 (2018).
22. D. D. Joshi, M. Puaud, M. Fouyssac, A. Belin-Rauscent, B. Everitt, D. Belin, The anterior insular cortex in the rat exerts an inhibitory influence over the loss of control of heroin intake and subsequent propensity to relapse. *Eur. J. Neurosci.* **52**, 4115–4126 (2020).
23. C. Silva, B. S. Porter, K. L. Hillman, Stimulation in the rat anterior insula and anterior cingulate during an effortful weightlifting task. *Front. Neurosci.* **15**, 643384 (2021).
24. J. L. Cadet, R. Patel, S. Jayanthi, Compulsive methamphetamine taking and abstinence in the presence of adverse consequences: Epigenetic and transcriptional consequences in the rat brain. *Pharmacol. Biochem. Behav.* **179**, 98–108 (2019).
25. R. Bock, J. H. Shin, A. R. Kaplan, A. Dobi, E. Markey, P. F. Kramer, C. M. Gremel, C. H. Christensen, M. F. Adrover, V. A. Alvarez, Strengthening the accumbal indirect pathway promotes resilience to compulsive cocaine use. *Nat. Neurosci.* **16**, 632–638 (2013).
26. E. A. Griffin Jr., P. A. Melas, R. Zhou, Y. Li, P. Mercado, K. A. Kempadoo, S. Stephenson, L. Colnaghi, K. Taylor, M. C. Hu, E. R. Kandel, D. B. Kandel, Prior alcohol use enhances vulnerability to compulsive cocaine self-administration by promoting degradation of HDAC4 and HDAC5. *Sci. Adv.* **3**, 1701682 (2017).
27. C. Giuliano, D. Belin, B. J. Everitt, Compulsive alcohol seeking results from a failure to disengage dorsolateral striatal control over behavior. *J. Neurosci.* **39**, 1744–1754 (2019).
28. A. Belin-Rauscent, M. L. Daniel, M. Puaud, B. Jupp, S. Sawiak, D. Howett, C. McKenzie, D. Caprioli, M. Besson, T. W. Robbins, B. J. Everitt, J. W. Dalley, D. Belin, From impulses to maladaptive actions: The insula is a neurobiological gate for the development of compulsive behavior. *Mol. Psychiatry* **21**, 491–499 (2016).
29. E. N. Grodin, C. R. Cortes, P. A. Spagnolo, R. Momenan, Structural deficits in salience network regions are associated with increased impulsivity and compulsivity in alcohol dependence. *Drug Alcohol Depend.* **179**, 100–108 (2017).
30. H. Chen, A. W. Lasek, Perineuronal nets in the insula regulate aversion-resistant alcohol drinking. *Addict. Biol.* **25**, e12821 (2020).
31. M. P. Paulus, J. L. Stewart, Interoception and drug addiction. *Neuropharmacology* **76**, 342–350 (2014).
32. L. Quadt, H. D. Critchley, S. N. Garfinkel, The neurobiology of interoception in health and disease. *Ann. N. Y. Acad. Sci.* **1428**, 112–128 (2018).
33. M. Contreras, F. Ceric, F. Torrealba, Inactivation of the interoceptive insula disrupts drug craving and malaise induced by lithium. *Science* **318**, 655–658 (2007).
34. L. Wang, H. Yu, J. Hu, J. Theeuwes, X. Gong, Y. Xiang, C. Jiang, X. Zhou, Reward breaks through center-surround inhibition via anterior insula. *Hum. Brain Mapp.* **36**, 5233–5251 (2015).
35. M. C. M. Gueguen, A. Lopez-Persem, P. Billeke, J. P. Lachaux, S. Rheims, P. Kahane, L. Minotti, O. David, M. Pessiglione, J. Bastin, Anatomical dissociation of intracerebral signals for reward and punishment prediction errors in humans. *Nat. Commun.* **12**, 3344 (2021).
36. H. Ishii, S. Ohara, P. N. Tobler, K. Tsutsui, T. Iijima, Inactivating anterior insular cortex reduces risk taking. *J. Neurosci.* **32**, 16031–16039 (2012).
37. A. Yiannakas, S. Kolatt Chandran, H. Kayyal, N. Gould, M. Khamaisy, K. Rosenblum, Parvalbumin interneuron inhibition onto anterior insula neurons projecting to the basolateral amygdala drives aversive taste memory retrieval. *Curr. Biol.* **31**, 2770–2784.e6 (2021).
38. T. De Oliveira Sergio, K. Lei, C. Kwok, S. Ghotra, S. A. Wegner, M. Walsh, J. Waal, D. Darevsky, F. W. Hopf, The role of anterior insula-brainstem projections and alpha-1 noradrenergic receptors for compulsion-like and alcohol-only drinking. *Neuropsychopharmacology* **46**, 1918–1926 (2021).
39. F. Lucantonio, Y. K. Takahashi, A. F. Hoffman, C. Y. Chang, S. Bali-Chaudhary, Y. Shaham, C. R. Lupica, G. Schoenbaum, Orbitofrontal activation restores insight lost after cocaine use. *Nat. Neurosci.* **17**, 1092–1099 (2014).
40. T. A. Stalnaker, N. K. Cooch, G. Schoenbaum, What the orbitofrontal cortex does not do. *Nat. Neurosci.* **18**, 620–627 (2015).
41. Y. Bi, Y. Zhang, Y. Li, D. Yu, K. Yuan, J. Tian, 12 h abstinence-induced right anterior insula network pattern changes in young smokers. *Drug Alcohol Depend.* **176**, 162–168 (2017).
42. M. E. Halcomb, E. J. Chumin, J. Goñi, M. Dzemidzic, K. K. Yoder, Aberrations of anterior insular cortex functional connectivity in nontreatment-seeking alcoholics. *Psychiatry Res. Neuroimaging* **284**, 21–28 (2019).
43. C. Wang, S. Wang, P. Huang, Z. Shen, W. Qian, X. Luo, K. Li, Q. Zeng, Q. Gu, H. Yu, Y. Yang, M. Zhang, Abnormal white matter tracts of insula in smokers. *Brain Imaging Behav.* **15**, 1955–1965 (2021).
44. E. D. Claus, S. K. Blaine, F. M. Filbey, A. R. Mayer, K. E. Hutchison, Association between nicotine dependence severity, BOLD response to smoking cues, and functional connectivity. *Neuropsychopharmacology* **38**, 2363–2372 (2013).
45. Y. Hu, B. J. Salmeron, I. N. Krasnova, H. Gu, H. Lu, A. Bonci, J. L. Cadet, E. A. Stein, Y. Yang, Compulsive drug use is associated with imbalance of orbitofrontal- and prelimbic-striatal circuits in punishment-resistant individuals. *Proc. Natl. Acad. Sci. U.S.A.* **116**, 9066–9071 (2019).
46. E. A. Murray, E. J. Moylan, K. S. Saleem, B. M. Basile, J. Turchi, Specialized areas for value updating and goal selection in the primate orbitofrontal cortex. *eLife* **4**, 11695 (2015).
47. L. K. Fellows, Orbitofrontal contributions to value-based decision making: Evidence from humans with frontal lobe damage. *Ann. N. Y. Acad. Sci.* **1239**, 51–58 (2011).
48. H. Seo, D. Lee, Orbitofrontal cortex assigns credit wisely. *Neuron* **65**, 736–738 (2010).
49. W. Sun, M. B. Yuill, Role of the GABA(a) and GABA(b) receptors of the central nucleus of the amygdala in compulsive cocaine-seeking behavior in male rats. *Psychopharmacology* **237**, 3759–3771 (2020).
50. Y. Bai, L. T. Ma, Y. B. Chen, D. Ren, Y. B. Chen, Y. Q. Li, H. K. Sun, X. T. Qiu, T. Zhang, M. M. Zhang, X. N. Yi, T. Chen, H. Li, B. Y. Fan, Y. Q. Li, Anterior insular cortex mediates hyperalgesia induced by chronic pancreatitis in rats. *Mol. Brain* **12**, 76 (2019).
51. Y. X. Xue, Y. Y. Chen, L. B. Zhang, L. Q. Zhang, G. D. Huang, S. C. Sun, J. H. Deng, Y. X. Luo, Y. P. Bao, P. Wu, Y. Han, B. T. Hope, Y. Shaham, J. Shi, L. Lu, Selective inhibition of amygdala neuronal ensembles encoding nicotine-associated memories inhibits nicotine preference and relapse. *Biol. Psychiatry* **82**, 781–793 (2017).
52. J. R. Deuis, L. S. Dvorakova, I. Vetter, Methods used to evaluate pain behaviors in rodents. *Front. Mol. Neurosci.* **10**, 284 (2017).
53. J. H. Deng, W. Yan, Y. Han, C. Chen, S. Q. Meng, C. Y. Sun, L. Z. Xu, Y. X. Xue, X. J. Gao, N. Chen, F. L. Zhang, Y. M. Wang, J. Shi, L. Lu, Predictable chronic mild stress during adolescence promotes fear memory extinction in adulthood. *Sci. Rep.* **7**, 7857 (2017).
54. Y. Chen, L. Zhang, Z. Ding, X. Wu, G. Wang, J. Shi, Effects of 3-methylmethcathinone on conditioned place preference and anxiety-like behavior: Comparison with methamphetamine. *Front. Mol. Neurosci.* **15**, 975820 (2022).
55. Q. Guo, J. Zhou, Q. Feng, R. Lin, H. Gong, Q. Luo, S. Zeng, M. Luo, L. Fu, Multi-channel fiber photometry for population neuronal activity recording. *Biomed. Opt. Express* **6**, 3919–3931 (2015).
56. J. W. de Jong, S. A. Afjei, I. Pollak Dorocic, J. R. Peck, C. Liu, C. K. Kim, L. Tian, K. Deisseroth, S. Lammel, A neural circuit mechanism for encoding aversive stimuli in the mesolimbic dopamine system. *Neuron* **101**, 133–151.e7 (2019).
57. C. C. Bavley, R. N. Fetcho, C. E. Burgdorf, A. P. Walsh, D. K. Fischer, B. S. Hall, N. M. Sayles, N. H. Contoreggi, J. E. Hackett, S. A. Antigua, R. Babij, N. V. De Marco Garcia, T. L. Kash, T. A. Milner, C. Liston, A. M. Rajadhyaksha, Cocaine- and stress-primed reinstatement of drug-associated memories elicit differential behavioral and frontostriatal circuit activity patterns via recruitment of L-type $Ca^{2+}$ channels. *Mol. Psychiatry* **25**, 2373–2391 (2020).
58. L. Y. Zhang, Y. Q. Zhou, Z. P. Yu, X. Q. Zhang, J. Shi, H. W. Shen, Restoring glutamate homeostasis in the nucleus accumbens via endocannabinoid-mimetic drug prevents relapse to cocaine seeking behavior in rats. *Neuropsychopharmacology* **46**, 970–981 (2021).



**Acknowledgments**

**Funding:** This study was funded by the Ministry of Science and Technology of China (2021ZD0202100), National Natural Science Foundation of China (U1802283, 82130040, and 82271533), and Beijing Municipal Science and Technology Commission (Z181100001518005).


**Author contributions:** Y.C., G.W., Y.X., and J.S. conceived the project. Y.C. performed the experiments. G.W., W.Z., L.Z., and Y.X. provided help with the experiments and experimental design. Y.H., H.X., S.M., L.L., and J.S. contributed to critical analysis of the data. Y.C. and G.W. wrote the manuscript, with input from all authors. **Competing interests:** The authors declare that they have no competing interests. **Data and materials availability:** All data needed to evaluate the conclusions in the paper are present in the paper and/or the Supplementary Materials.


Submitted 17 April 2022
Accepted 23 November 2022
Published 23 December 2022
10.1126/sciadv.abq5745